Biophysical Journal Volume 75 September 1998 1397–1402

Surface Specific Kinetics of Lipid Vesicle Adsorption Measured with a Quartz Crystal Microbalance

C. A. Keller and B. Kasemo

Department of Applied Physics, Chalmers University of Technology and Göteborg University, S-412 96 Göteborg, Sweden

ABSTRACT We have measured the kinetics of adsorption of small (12.5-nm radius) unilamellar vesicles onto SiO_2, oxidized gold, and a self-assembled monolayer of methyl-terminated thiols, using a quartz crystal microbalance (QCM). Simultaneous measurements of the shift in resonant frequency and the change in energy dissipation as a function of time provide a simple way of characterizing the adsorption process. The measured parameters correspond, respectively, to adsorbed mass and to the mechanical properties of the adsorbed layer as it is formed. The adsorption kinetics are surface specific; different surfaces cause monolayer, bilayer, and intact vesicle adsorption. The formation of a lipid bilayer on SiO_2 is a two-phase process in which adsorption of a layer of intact vesicles precedes the formation of the bilayer. This is, to our knowledge, the first direct evidence of intact vesicles as a precursor to bilayer formation on a planar substrate. On an oxidized gold surface, the vesicles adsorb intact. The intact adsorption of such small vesicles has not previously been demonstrated. Based on these results, we discuss the capacity of QCM measurements to provide information about the kinetics of formation and the properties of adsorbed layers.

INTRODUCTION

Supported membranes are currently receiving increasing attention. Scientifically they have proven invaluable in the study of the properties and function of membrane-bound proteins and, more generally, in the study of membrane-mediated processes such as cell-cell interactions (McConnell et al., 1986; Nollert et al., 1995) and biological signal transduction (Heyse et al., 1995). Practically, supported membranes allow the biofunctionalization of inorganic surfaces. Potential applications include biosensors, the acceleration and improvement of medical implant acceptance, programmed drug delivery, and the production of catalytic interfaces (Ebato et al., 1994; Sackmann, 1996; Tampé et al., 1996).

The immobilization of the membrane at a surface permits rapid exchange of the fluids in contact with the membrane. It allows the application of surface-sensitive probes such as surface plasmon resonance (SPR) (Ohlsson et al., 1995; Stelzle et al., 1993; Striebel et al., 1994), total internal reflection fluorescence microscopy (TIRFM) (Kalb et al., 1992), impedance spectroscopy (Steinem et al., 1996), and acoustic sensors such as the quartz crystal microbalance (QCM) (Ohlsson et al., 1995; Okahata and Ebato, 1989) and surface acoustic wave (SAW) devices (Gizeli et al., 1996). The intrinsically low bioactivity, i.e., low degree of nonspecific adsorptivity (Heyse et al., 1995; Janshoff et al., 1996; McConnell et al., 1986; Stelzle et al., 1993), of supported membranes makes them interesting as an interface between the nonbiological materials on the surface of a sensor or implant and biologically active fluids. Lipid membranes also provide a natural environment for the immobilization of bioactive molecules (Janshoff et al., 1996; Tampé et al., 1996) such as enzymes, antibodies, or antigens. These properties provide much of the motivation for using supported membranes in biosensors. The natural environment for the active molecules offered by lipid membranes preserves their high sensitivity and selectivity by preventing denaturation, the low bioactivity of the supporting membrane reduces spurious signals, and the localization of the active molecules at a surface aids in signal transduction.

Whereas much effort has been put into the production and characterization of different types of supported membranes, comparatively little work has been aimed at studying the processes by which they form (Brink et al., 1994; Feder et al., 1995; Heyse et al., 1995; Kalb et al., 1992; Lang et al., 1992, 1994; Seifert and Lipowsky, 1990; Steinem et al., 1996). For example, it is not known how small vesicles fuse with a surface to form a bilayer. Understanding of these processes is interesting for several reasons. These include developing an understanding of how complex molecular systems interact with surfaces (here lipid vesicles serve as a relatively simple model system) and of basic cellular process such as endocytosis and exocytosis (Seifert and Lipowsky, 1990). From a practical point of view, they are interesting because important structural and functional characteristics of a supported membrane, such as protein orientation (Salafsky et al., 1996), depend on the way it is formed from protein-containing vesicles.

Using recently developed techniques for measuring both the frequency and dissipation of the QCM (Rodahl et al., 1995), we have measured the kinetics of lipid vesicle adsorption onto different carefully prepared surfaces. The surfaces we discuss here are a self-assembled monolayer of methyl-terminated alkane thiols, oxidized gold, and silicon

Received for publication 15 December 1997 and in final form 27 May 1998.

Address reprint requests to Dr. Craig A. Keller or Prof. Bengt Kasemo, Department of Applied Physics, Chalmers University of Technology, S-412 96 Göteborg, Sweden. Tel.: 46-31-772-3396; Fax: 46-31-772-3134; E-mail: craigk@fy.chalmers.se.

0006-3495/98/09/1397/06 $2.00

dioxide. We present the first use of combined frequency and dissipation QCM measurements to study lipid membranes, and we demonstrate the capacity of this technique to distinguish different types of surface-specific adsorption kinetics and to determine the properties of the completed membrane.

MATERIALS AND METHODS

Materials

Milli-Q water (Millipore, Molsheim, France) was used for the final cleaning of the cell, for the preparation of the surfaces, and for all solutions. The buffer and electrolyte referred to as buffer throughout this paper is 10 mM Tris, pH 8.0, and 100 mM NaCl. The dye-lipid probe referred to as Texas Red DHPE is *N*-(Texas Red sulfonyl)-1,2-dihexadecanoyl-*sn*-glycero-3-phosphoethanolamine, triethylammonium salt (Molecular Probes, Eugene, OR). Other materials include silicon dioxide for evaporation (Balzers Process Systems, Sweden), octadecylmercaptan (Aldrich) for preparation of a methyl-terminated self-assembled monolayer (SAM), pro analysi grade chloroform (Merck), and high-performance liquid chromatography–grade hexane (Fisher). The 5 MHz quartz crystal microbalance sensors are polished 25.4-mm crystals with gold-on-chromium electrodes (Maxtek, Torrance, CA).

Preparation of lipid vesicles

Small unilamellar vesicles (SUVs) were prepared according to the protocol given by Salafsky et al. (Barenholz et al., 1977; Salafsky et al., 1996). Egg phosphatidylcholine (EggPC) (Sigma) was mixed with 1 mol% Texas red DHPE in chloroform. Under flowing nitrogen, the lipid mixture was dried onto the walls of a continuously rolled test tube, and then left for several hours to ensure the removal of all of the solvent. The dried lipids were resuspended in buffer by vortexing under a nitrogen atmosphere for ~30 min. Lipid vesicles were formed by sonicating the suspension to clarity, using the 1/8-inch microtip of a Branson probe sonicator. To prevent heating of the sample, the sonication was carried out on ice in 5-s pulses separated by 5-s cooling periods. The total sonication time was typically 60 min. The vesicle suspension was then spun at 150,000 $\times$ *g* for 4.5 h to separate the SUVs from larger lipid structures. After centrifugation, the supernatant above the pellet was drawn off in three fractions, and the lipid concentration in each fraction was determined by measuring the adsorption of the Texas Red dye. All of the work presented in this paper was performed with the second fraction, the lipid concentration of which (16.0 mM) lay between that of the first and third fractions. The SUV fractions were stored under N_2 in small vials at 4°C and were used over a 6-month period. Over this time period there were no qualitative changes in the adsorption behavior of the SUVs on any of the tested surfaces.

The hydrodynamic radius of the vesicles measured by photon correlation spectroscopy (PCS) was 12.5 $\pm$ 0.4 nm. The width of the distribution was very narrow, lying below the resolution of our experiments. This measurement agrees with previous work in which SUVs were prepared with the same protocol (Barenholz et al., 1977; Huang, 1969). The lateral mobility of the lipids in the bilayers on SiO_2 was verified by fluorescence recovery after photobleaching (FRAP) (Groves and Boxer, 1995; Salafsky et al., 1996). In agreement with previous work (Nollert et al., 1995), we find that any exposure to air destroys the bilayer.

Preparation of surfaces

Silicon dioxide

The surface of a QCM crystal was cleaned by briefly etching in an oxygen plasma (reactive ion etching) before the evaporation onto the surface of 3 nm of Ti as an adhesion layer followed by 100 nm of SiO_2. XPS analysis showed that this procedure produces a clean SiO_2 surface. After measuring lipid vesicle adsorption onto the surface, the crystals were soaked in a mild detergent solution for several hours and then rinsed with water, dried under N_2, and stored. Immediately before each use, the surface was cleaned with two cycles of the following procedure: exposure to UV-produced ozone in air at atmospheric pressure for 10 min, rinsing with water, and drying under N_2.

Thiolated gold

The gold electrodes on the QCM crystals were prepared for thiolation by immersing the crystals in a 5:1:1 solution of H_2O:H_2O_2(30%):NH_3(25%) at 80°C for 10 min, rinsing with water, and drying under N_2. After cleaning, the crystals were immediately immersed in ~1 mM octadecylmercaptan in hexane and left overnight. Immediately before use the crystals were removed from the thiolation bath; rinsed with hexane, ethanol, and water in succession; and dried under N_2.

Oxidized gold

The gold electrodes on the QCM crystals were prepared for oxidation by the same cleaning procedure as before thiolation. Immediately before use, the gold electrode was oxidized (Krozer and Rodahl, 1997) with two cycles of the following procedure: exposure to UV ozone for 10 min, rinsing with water, and drying under N_2. Krozer and Rodahl (1997) have characterized this surface by XPS and contact angle measurements. The former shows the presence of gold oxide and chemisorbed oxygen, and the latter gives a contact angle of less than 5°.

Preparation of the measurement cell

Before each set of data runs, the fluid cell was cleaned by filling it with a 2% solution of Hellmanex II, leaving it for at least 1 h, and then repeatedly rinsing with water. Between subsequent runs using the same vesicle preparation, the cell was repeatedly rinsed with water. With this procedure the character and amplitude of the frequency and dissipation shifts for the first and subsequent runs were identical, but the kinetics were consistently slower during the first run. The second and later runs were identical. We believe that during the first run lipid adsorption on the surfaces of the fluid cell and the liquid handling system lowered the concentration of vesicles in solution, causing the adsorption to occur at a slower rate. Runs with a lower initial vesicle concentration displayed the same behavior. Rinsing with Millipore water did not remove the adsorbed lipids from the cell walls, and thus the depletion of the solution was blocked in subsequent runs. Because of this, we generally used the first run on any given day to check that adsorption on SiO_2 reproduced previous measurements. This allowed us to check for any effects of aging of the vesicle preparation, for contamination of the buffer, and for cleanliness of the measurement cell.

Measurement of adsorption kinetics

Our measurement system is shown schematically in Fig. 1. The QCM crystal is mounted in a fluid cell that also provides temperature control to better than $\pm$0.05°C. Exchange of the fluid in the cell is accomplished by gravity feed from a 3-ml temperature-controlled reservoir directly above the cell. The exchange is controlled by a single valve. Immediately upon completion of the final surface preparation step, the QCM crystal was mounted in the fluid cell and exposed to clean buffer. After the measurement system was tuned to the resonant frequency of the crystal, the buffer was exchanged at least twice—each time by allowing 2 ml of buffer to flow through the cell—to check for contamination and to ensure that the measurements were begun from a stable baseline. The adsorption measurements presented here were begun by replacing the buffer with SUVs diluted in buffer to a concentration of 140 μM (0.10 mg/ml). Exchanging buffer for buffer or buffer for sample takes ~1 s and causes a transient

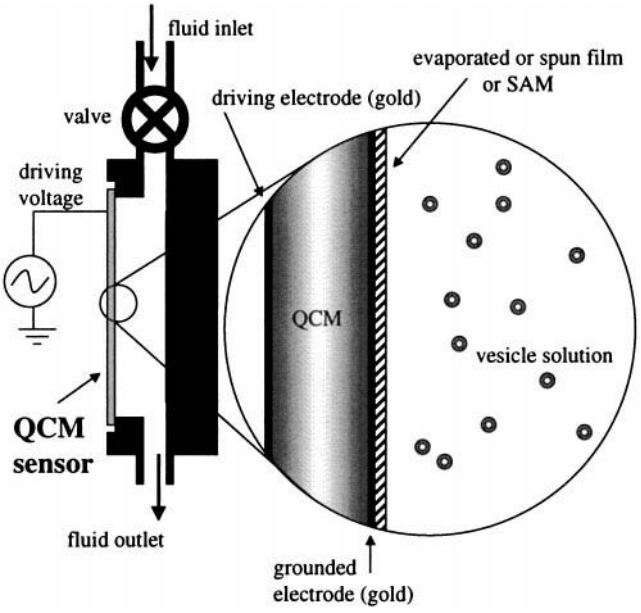

FIGURE 1 Schematic of the QCM crystal mounted in the fluid cell.

spike in the measured frequency and dissipation. The transient recovers within a few seconds and does not affect the baseline of the measurement. To minimize the fluid exchange transients and thermal drift, the fluid cell, buffer, and samples were all maintained at a constant temperature of 21.8°C. A set of rinses with clean buffer were performed after the adsorption was complete to check the stability of the adsorbed layer. After rinsing, the adsorbed layers have been stable for as long as we have monitored them (~1 h on each surface). For the 5-MHz QCM crystals used in this study, a frequency shift of 1 Hz corresponds to an adsorbed mass of 18 ng/cm^2. For comparison, the adsorption of a complete lipid monolayer corresponds to a frequency shift of 13 Hz. Repeated measurements of adsorption on SiO_2 show some variability in the time required to complete the adsorption of a complete bilayer (76–93 s) and in the maximum dissipation shift ($1.2–2.0 \times 10^{-6}$), whereas the total frequency shift after completion of the bilayer was reproducible to within ±0.5 Hz, and the peak in the frequency shift (see Fig. 2) showed little variation (60–68 Hz). We have yet to determine the source of these variations.

RESULTS AND DISCUSSION

Fig. 2 shows the measured frequency and dissipation shifts as a function of time for the adsorption of SUVs on three different surfaces—on a self-assembled monolayer of methyl-terminated thiols on gold, on SiO_2, and on oxidized gold. The first surface is extremely hydrophobic because of its —CH_3 termination, whereas the latter two are quite hydrophilic. For each surface, the measurements are plotted on identical scales.

SiO_2: bilayer adsorption

Once the adsorption of SUVs of EggPC onto SiO_2 is complete, the total frequency shift is 26.0 Hz and no further adsorption is observed (Kalb et al., 1992). For the QCM crystals we use, this corresponds to an adsorbed mass of 468 ng/cm^2. Dividing this into the molecular mass of the lipid molecule (768 Da; Huang and Mason, 1978) and assuming a bilayer topology gives a surface area per molecule of 55 Å^2. This is consistent with the formation of a bilayer, although somewhat smaller than the 66–69 Å^2 indicated in previous work (Huang and Mason, 1978). The difference may be accounted for by our neglect of the hydration of the lipid molecules and the mass of the thin layer of water that is thought to exist between the bilayer and the surface (Johnson et al., 1991). Our observations are consistent with

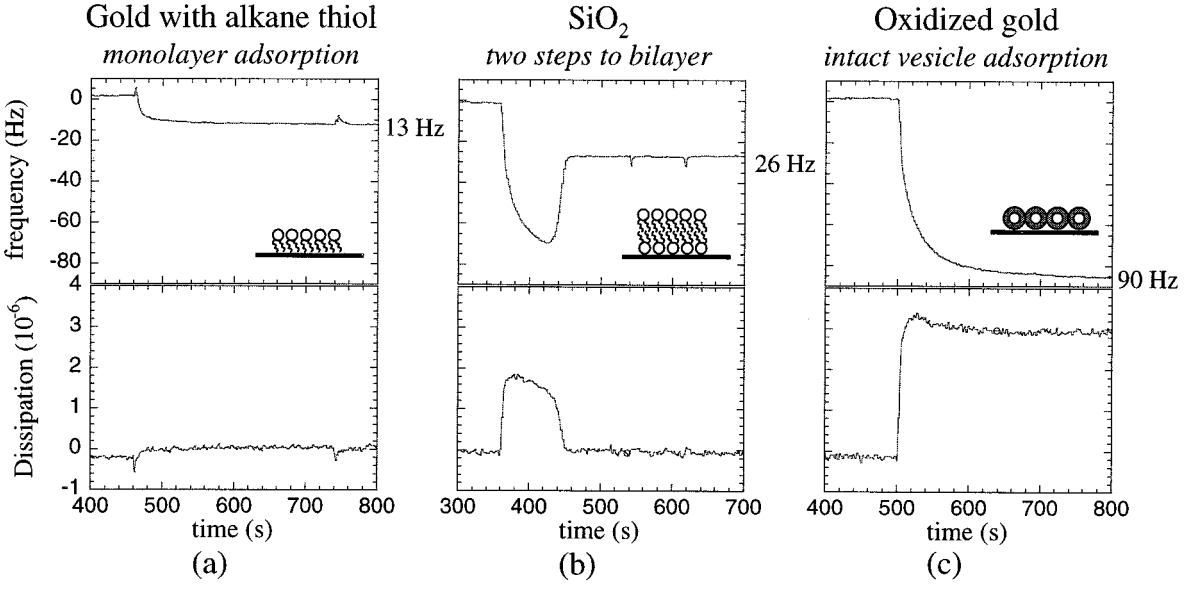

FIGURE 2 Change in QCM resonant frequency and dissipation versus time for the adsorption of SUVs onto (*a*) gold with a SAM of methyl terminated alkane thiols, (*b*) silicon dioxide, and (*c*) oxidized gold. Note that the time, frequency, and dissipation scales for the three sets of data are identical. Rinses occurred at the spikes at 740 s in *a* and at 541 s and 616 s in *b*. The inset in each frequency versus time plot is a schematic depiction of the adsorbed layer as deduced from the experimental results. These pictures are not to scale.

previous work that has shown that SUVs of EggPC adsorb as a bilayer on SiO_2 (Brian and McConnell, 1984; Salafsky et al., 1996). Note that once the adsorption of the bilayer is complete, there is no net change in the measured dissipation. The interesting nonmonotonic adsorption kinetics (Fig. 2 *b*) will be discussed later.

Methyl-terminated SAM: monolayer adsorption

The adsorption of SUVs onto a SAM of methyl-terminated thiols displays the simple exponential behavior characteristic of adsorption of a monolayer by first-order kinetics. The total frequency shift (13.0 Hz) is half of that observed for bilayer adsorption, indicating the formation of a lipid monolayer. If we consider the hydrophobic interaction to be the primary driving force, this is exactly what is expected energetically for the adsorption of an amphiphilic molecule onto a hydrophobic surface in an aqueous solution. Note that no change in dissipation occurs during the adsorption process.

Oxidized gold: adsorption of intact vesicles

When EggPC SUVs are adsorbed onto an oxidized gold surface, there is a large shift in the resonant frequency (seven times larger than on the methyl-terminated thiol surface) accompanied by a large shift in the dissipation. We attribute this to the adsorption of a close-packed layer of intact lipid vesicles. Three observations support this interpretation: 1) The large frequency shift (90.0 Hz) corresponds to that expected for the adsorption of lipid vesicles with a radius of 12.5 nm. 2) The adsorption rapidly saturates at a consistent value that is unaffected by rinsing. 3) The large dissipation shift indicates that the structure of the adsorbed film is fundamentally different from either an adsorbed monolayer or an adsorbed bilayer.

Now we discuss each of these observations in a little more detail. First we estimate the frequency shift. The total mass of a layer of intact vesicles can be estimated by assuming that the layer is formed of close-packed spheres, including the mass of the buffer within the vesicles, and including the mass of the buffer trapped between the vesicles and the surface; the last is estimated by including the pore volume between the spheres that lies between a plane through the center of the spheres and the plane of the surface. The result is an added mass of 1.38 $\mu g/cm^2$ for the spheres and the buffer inside of them and 0.536 $\mu g/cm^2$ for the buffer trapped below the midline of the spheres. These estimates correspond to a total frequency shift of 107 Hz. This is slightly larger than the measured frequency shift of 90 Hz. The difference can be attributed to our assumptions that the layer of vesicles is close-packed without defects, that the vesicles do not experience any flattening when adsorbed on the surface, and that the frequency shift of the QCM is strictly proportional to the mass, even when a large dissipation shift is observed (Voinova et al., manuscript submitted for publication). Any deviation from these assumptions will result in over estimation of the adsorbed mass. Together the rapid saturation of the adsorption, the stability of the adsorbed layer to rinsing, and the lack of multilayer adsorption after the adsorption of a monolayer or a bilayer on the other surfaces treated in this paper suggest that the observed adsorption is not due to the formation of multilayers (Ohlsson et al., 1995) or to the adsorption of an amorphous layer whose thickness is determined by an equilibrium between adsorption and desorption. All of our observations are consistent with the irreversible adsorption of a dense monolayer of intact lipid vesicles on oxidized gold.

The large dissipation shift seen for the adsorption of intact SUVs on oxidized gold is in striking contrast to the lack of dissipation shift for either a completely formed bilayer or a monolayer. This reflects the intrinsically different structure of the adsorbed layer on oxidized gold, and highlights the utility of measuring both the frequency and dissipation shifts during adsorption. Both the lipid bilayer and the lipid monolayer are very compact structures lying close to the surface of the QCM, where they couple strongly to the motion of the crystal surface; this explains the absence of a measurable dissipation shift for these structures. Adsorbed vesicles are substantially larger and less compact structures and are thus subject to larger deformations under shear stress. Driving the shear motion of the outer surface of the adsorbed layer requires coupling of the motion of the QCM surface through the vesicles and into the fluid. This process can cause deformation of the vesicles, which via internal friction will cause an increase in the energy dissipation.

We believe that the intact vesicles on oxidized gold (12.5 nm radius) are the smallest vesicles that have been observed to adsorb intact on any surface (Nollert et al., 1995; Xia and Ven, 1992). These vesicles are much smaller than the critical radius ($R_C \approx 200$ nm) below which Seifert and Lipowsky (1990) predicted that vesicle binding will depend on a competition between the adhesive energy and the bending energy. They also predict that in this regime vesicles below a certain potential-dependent size will spontaneously unbind from the surface. The results presented here should provide a useful test case for this theory. The high polarizability of the gold surface maximizes the attractive potential, and as a consequence makes it not too surprising that such small vesicles adhere to the surface. What is surprising is that the strong attractive potential does not cause the vesicles to rupture.

Lipowsky and Seifert propose as part of their analysis of that vesicle rupture occurs when strong adhesive forces cause the tension in the membrane of the spherical cap of an adsorbing vesicle to exceed the threshold for disruption of the membrane; they also propose a mechanism for vesicle fusion on a surface (Lipowsky and Seifert, 1991). These mechanisms could explain why we see intact vesicles on oxidized gold and a bilayer formed from ruptured vesicles on SiO_2, except that both of these mechanisms predict that the outer surface of the vesicle becomes, primarily, the leaflet of the bilayer facing the surface. This contradicts

experiments by Salafsky et al. (1996) on the formation of bilayers from vesicles containing proteins (before the addition of the proteins their vesicle preparation is identical to ours). In their experiments, they showed that vesicles with 95% protein orientation produced a bilayer with 90% orientation. The end of the protein at the outer surface of the vesicle was oriented away from the surface.

We are currently performing experiments to look at the stability of a partially formed layer of vesicles and to determine the order of the adsorption kinetics. We have performed FRAP measurements on this surface, but the results were inconclusive because the fluorescence is almost completely quenched by the gold surface. We are performing further characterizations to confirm the intact adsorption of these vesicles.

Bilayer adsorption on SiO_2: adsorption kinetics

Probably the most striking aspect of the data shown in Fig. 2 *b* is the large peak in the frequency shift accompanied by a large maximum in the dissipation, which occurs during the adsorption of lipid vesicles on SiO_2. Nothing like this is seen in the adsorption of the SUVs on oxidized or thiolated gold. Comparing the initial adsorption behavior on SiO_2 to intact vesicle adsorption on oxidized gold strongly suggests that the formation of the lipid bilayer on SiO_2 is preceded by the adsorption of intact vesicles. Both adsorption measurements begin with a large and quantitatively similar decrease in the frequency, accompanied by a large and rapid increase in the dissipation. The initial similarity between the two adsorption events is born out by the similarity in plots of dissipation versus frequency during the initial adsorption (not shown). Precursor adsorption of intact vesicles has been used to explain observations of the formation of a second lipid layer on the hydrophobic surface of a lipid monolayer deposited by the Langmuir-Blodgett technique (Kalb et al., 1992) and to explain observations of adsorption on glass beads (Jackson et al., 1987). Coexistence of ruptured and intact vesicles on MgF_2 has also been observed (Rädler et al., 1995). The experiment of Kalb et al. is especially interesting. Using FRAP, they observed the sudden onset of lateral diffusion in the adsorbed lipid layer at a critical lipid surface concentration. They suggest that this is due to the adsorption of intact vesicles onto the supported lipid monolayer. The measurements on SiO_2 presented here are direct evidence for such precursors in the formation of a planar bilayer from vesicles.

This picture brings two time scales to attention, one for intact vesicle adsorption and one for the breaking and spreading of the vesicles to form a bilayer. On the methyl-terminated thiol surface, the breaking and spreading of the lipid vesicles to form a simple monolayer is obviously very fast, and the lifetime of intact vesicles is very short. On oxidized gold, the reverse applies; the lifetime of intact vesicles is effectively infinite on the time scale of the experiment ($\sim$1 h). The adsorption of vesicles on SiO_2 occurs at a rate that is of the same order of magnitude but somewhat faster than the time required to break and spread the vesicles. To test this we have looked at the adsorption of SUVs onto SiO_2 from SUV solutions of different concentrations. We found that the rate of the initial mass uptake and the rate at which the system thinned to a bilayer both changed with concentration. Both rates increased as the concentration increased. Because a vesicle needs to adsorb before it can break, there is obviously a coupling between the two processes, but our measurements suggest that the coupling is quite complex, because the magnitude of the peak in the frequency shift did not change with the concentration of the vesicle solution. Further measurements and modeling are being performed in an attempt to clarify the relationship between the adsorption of vesicles on the surface and the rate of breaking and spreading.

CONCLUSIONS

We have demonstrated that simultaneous frequency and dissipation measurements performed with the QCM are a very effective means of measuring the kinetics of lipid vesicle adsorption and of characterizing the adsorbed layers.

Our measurements demonstrate that lipid vesicle adsorption occurs in a qualitatively different manner on each of thiolated gold, SiO_2, and oxidized gold, that bilayer adsorption on SiO_2 is preceded by the adsorption of a layer of intact vesicles, and that, on an oxidized gold surface, the irreversible, stable adsorption of 25-nm-diameter vesicles is possible.

We thank Julie Gold for the XPS analysis, Peter Brzezinski for access to biochemical preparation facilities, Fredrik Höök for his help in the laboratory, and Michael Rodahl, Duncan Sutherland, and Jay Groves for many useful discussions.

This work was done with financial support from the Swedish Biomaterials Consortium Swedish National Board for Industrial and Technical Development (NUTEK) and Swedish Natural Science Research Council (NFR) contract 96-12064) and Swedish Research Council for Engineering Sciences (TFR) (contract 95-782).

REFERENCES

Barenholz, Y., D. Gibbes, B. J. Litman, J. Goll, T. E. Thompson, and F. D. Carlson. 1977. A simple method for the preparation of homogeneous phospholipid vesicles. *Biochemistry.* 16:2806–2810.

Brian, A. A., and H. M. McConnell. 1984. Allogeneic stimulation of cytotoxic T cells by supported planar membranes. *Proc. Natl. Acad. Sci. USA.* 81:6159–6163.

Brink, G., L. Schmitt, R. Tampé, and E. Sackmann. 1994. Self assembly of covalently anchored phospholipid supported membranes by use of DODA-Suc NHS-lipids. *Biochim. Biophys. Acta.* 1196:227–230.

Ebato, H., C. A. Gentry, J. N. Herron, W. Müller, Y. Okahata, H. Ringsdorf, and P. A. Suci. 1994. Investigation of specific binding of antifluorescyl antibody and Fab to fluorescein lipids in Langmuir-Blodgett deposited films using quartz crystal microbalance methodology. *Anal. Chem.* 66:1683–1689.

Feder, T. J., G. Weissmüller, B. Zekö, and E. Sackmann. 1995. Spreading of giant vesicles on moderately adhesive substrates by fingering: a reflection interference contrast microscopy study. *Phys. Rev. E.* 51: 3427–3433.

Gizeli, E., C. R. Lowe, M. Liley, and H. Vogel. 1996. Detection of supported lipid layers with the acoustic Love waveguide device: application to biosensors. *Sensors Actuators B.* 34:295–300.

Groves, J. T., and S. G. Boxer. 1995. Electric field-induced concentration gradients in planar supported bilayers. *Biophys. J.* 69:1972–1975.

Heyse, S., H. Vogel, M. Sänger, and H. Sigrist. 1995. Covalent attachment of functionalized lipid bilayers to planar waveguides for measuring protein binding to biomimetic membranes. *Protein Sci.* 4:2532–2544.

Huang, C.-H. 1969. Studies on phosphatidylcholine vesicles. Formation and physical characteristics. *Biochemistry.* 8:344–352.

Huang, C., and J. T. Mason. 1978. Geometric packing constraints in egg phosphatidylcholine vesicles. *Proc. Natl. Acad. Sci. USA.* 75:308–310.

Jackson, S. M., M. D. Reboiras, I. G. Lyle, and M. N. Jones. 1987. The mechanism of phospholipid adsorption from vesicle dispersions onto glass surfaces. *Colloids Surfaces.* 27:325–340.

Janshoff, A., C. Steinem, M. Sieber, and H.-J. Galla. 1996. Specific binding of peanut agglutinin to G_{M1}-doped solid supported lipid bilayers investigated by shear wave resonator measurements. *Eur. Biophys. J.* 25:105–113.

Johnson, S. J., T. M. Bayerl, D. C. McDermott, G. W. Adam, A. R. Rennie, R. K. Thomas, and E. Sackmann. 1991. Structure of an adsorbed dimyristoylphosphatidylcholine bilayer measured with specular reflection of neutrons. *Biophys. J.* 59:289–294.

Kalb, E., S. Frey, and L. K. Tamm. 1992. Formation of supported planar bilayers by fusion of vesicles to supported phospholipid monolayers. *Biochim. Biophys. Acta.* 1103:307–316.

Krozer, A., and M. Rodahl. 1997. X-ray photoemission spectroscopy study of UV/ozone oxidation of Au under UHV conditions. *J. Vac. Sci. Tech. A.* 15:1704–1709.

Lang, H., C. Duschl, M. Grätzel, and H. Vogel. 1992. Self-assembly of thiolipid molecular layers on gold surfaces: optical and electrochemical characterization. *Thin Solid Films.* 210/211:818–821.

Lang, H., C. Dushchl, and H. Vogel. 1994. A new class of thiolipids for the attachment of lipid bilayers on gold surfaces. *Langmuir.* 10:197–210.

Lipowsky, R., and U. Seifert. 1991. Adhesion of vesicles and membranes. *Mol. Crystals.* 202:17–25.

McConnell, H. M., T. H. Watts, R. M. Weis, and A. A. Brian. 1986. Supported planar membranes in studies of cell-cell recognition. *Biochim. Biophys. Acta.* 864:95–106.

Nollert, P., H. Kiefer, and F. Jähnig. 1995. Lipid vesicle adsorption versus formation of planar bilayers on solid surfaces. *Biophys. J.* 69: 1447–1455.

Ohlsson, P.-Å., T. Tjärnhage, E. Herbai, S. Löfås, and G. Puu. 1995. Liposome and proteoliposome fusion onto solid substrates, studied using atomic force microscopy, quartz crystal microbalance and surface plasmon resonance. Biological activities of incorporated components. *Bioelectrochem. Bioenerg.* 38:137–148.

Okahata, Y., and H. Ebato. 1989. Application of a quartz-crystal microbalance for detection of phase transitions in liquid crystals and lipid multibilayers. *Anal. Chem.* 61:2185–2188.

Rädler, J., H. Strey, and E. Sackmann. 1995. Phenomenology and kinetics of lipid bilayer spreading on hydrophilic surfaces. *Langmuir.* 11: 4539–4548.

Rodahl, M., F. Höök, A. Krozer, P. Brzezinski, and B. Kasemo. 1995. Quartz crystal microbalance setup for frequency and Q-factor measurements in gaseous and liquid environments. *Rev. Sci. Instrum.* 66: 3924–3930.

Sackmann, E. 1996. Supported membranes: scientific and practical applications. *Science.* 271:43–48.

Salafsky, J., J. T. Groves, and S. G. Boxer. 1996. Architecture and function of membrane proteins in planar supported bilayers: a study with photosynthetic reaction centers. *Biochemistry.* 35:14773–14781.

Seifert, U., and R. Lipowsky. 1990. Adhesion of vesicles. *Phys. Rev. A.* 42:4768–4771.

Steinem, C., A. Janshof, W.-P. Ulrich, M. Sieber, and H.-J. Galla. 1996. Impedance analysis of supported lipid bilayer membranes: a scrutiny of different preparation techniques. *Biochim. Biophys. Acta.* 1279: 169–180.

Stelzle, M., G. Weissmüller, and E. Sackmann. 1993. On the application of supported bilayers as receptive layers for biosensors with electrical detection. *J. Phys. Chem.* 97:2974–2981.

Striebel, C., A. Brecht, and G. Gauglitz. 1994. Characterization of biomembranes by spectral ellipsometry, surface plasmon resonance and interferometry with regard to biosensor application. *Biosens. Bioelectron.* 9:139–146.

Tampé, R., C. Dietrich, S. Gritsch, G. Elender, and L. Schmitt. 1996. Biofunctionalized membranes on solid surfaces. *In* Nanofabrication and Biosystems. H. C. Hoch, L. W. Jelinsi, and H. G. Craighead, editors. Cambridge University Press, Cambridge. 201–221.

Xia, Z., and T. G. M. v. d. Ven. 1992. Adhesion kinetics of phosphatidylcholine liposomes by evanescent wave light scattering. *Langmuir.* 8:2938–2946.